PCCP

Influence of aqueous solutions of 2-(tetrafluoro(trifluoromethyl)-λ^6-sulfanyl-ethan-1-ol (CF_3SF_4-ethanol) on the stabilization of the secondary structure of melittin: Comparison with aqueous trifluoroethanol using molecular dynamics simulations and circular dichroism experiments.

Journal:	*Physical Chemistry Chemical Physics*
Manuscript ID	CP-ART-07-2024-002654.R1
Article Type:	Paper
Date Submitted by the Author:	26-Nov-2024
Complete List of Authors:	Biswas, Samadrita; University at Albany, Chemistry Pathak, Nilavra; Expedia Group, Marketing Data Science Sutherland, Leah; University at Albany, Chemistry Chen, Alan; University at Albany, SUNY, Chemistry/RNA Institute; University at Albany, Welch, John; University at Albany, Chemistry

PAPER

Influence of aqueous solutions of 2-(tetrafluoro(trifluoromethyl)-λ⁶-sulfanyl-ethan-1-ol (CF_3SF_4-ethanol) on the stabilization of the secondary structure of melittin: Comparison with aqueous trifluoroethanol using molecular dynamics simulations and circular dichroism experiments.

Received 00th January 20xx,
Accepted 00th January 20xx

DOI: 10.1039/x0xx00000x

Samadrita Biswas,*[a] Nilavra Pathak [b], Leah Sutherland[a], Alan A Chen[c] and John T Welch [a]

The influence of aqueous solutions of 2-(tetrafluoro(trifluoromethyl)-λ⁶-sulfanyl-ethan-1-ol (CF_3SF_4-ethanol) and 2,2,2-trifluoroethanol (TFE), on the secondary structure of melittin was studied using circular dichroism (CD) and molecular dynamics (MD) simulations. In water, melittin transitions to a random coil. However, on the addition of even as little as 1% by volume of CF_3SF_4-ethanol, the secondary structure of melittin stabilizes as helix. Contrarily, the addition of 40% by volume of TFE is required for the greatest helicity . Fluoroalcohols stabilize melittin's hydrophobic side chain residues thereby enhancing the helical structure. Locally alcohol concentrations approach nearly 70-90% in the near vicinity of the hydrophobic side chains increasing hydrophobic interactions and reducing water-peptide hydrogen bonding. Using the Molecular Mechanics-Poisson Boltzmann Surface Area method (MMPBSA), the free energy of binding between the peptide and fluoroalcohols highlighted the role of nonpolar residues on stabilization of the secondary structure. Secondary Structure Content Analysis (SESCA) validated the simulation results, confirming CF_3SF_4-ethanol as an effective, eco-friendly enhancer of helicity at low concentrations. The far UV circular dichroism (CD) of melittin in solutions containing TFE corroborate previous findings and likewise affirm that the addition of CF_3SF_4-ethanol to an aqueous solution can enhance helicity. The agreement between experimental and calculated helicities highlights the potential of CF_3SF_4-ethanol. This study offers insights into peptide stabilization by fluoroalcohols, with implications for peptide-based therapeutic design.

Introduction

Fluoroalcohols are effective cosolvents widely used for the secondary structure stabilization of peptides.[1-7] In particular, 2,2,2-trifluoroethanol (TFE) was one of the most effective helix-inducing and stabilizing cosolvents.[1, 8-12] Mechanism of peptide stabilization by fluorinated solvents has been investigated experimentally using circular dichroism, NMR and by molecular dynamics simulations.[1, 4, 7, 12-24] These studies highlight the complex interactions that involve a combination of different effects. As a solute TFE can perturb the structure of water, dramatically lowering the dielectric constant of the solution while promoting preferential hydrophobic solvation.[25] Additionally, it can form hydrogen bonds with the backbone of the protein.[26] Molecular dynamics simulations indicated a cosolvent induced a coating effect on the simulated peptides as a possible mechanism of peptide stabilization. The coating effect is favored by the tendency of the fluorinated solvents to form large clusters in aqueous solution.[12] The cosolvent layer surrounding the peptide decreases the exposure of the backbone hydrogen bonds to the water, which, in turn, reduces bonding between water and the peptide backbone.[12] Because of this plethora of effects on the solution structure and interactions, the role of TFE on the stabilization of helices is difficult to rationalize.

Among the peptides used to experimentally study the effects of fluorinated solvents, melittin (MLT) was one of the most frequently investigated. Melittin is a 26-amino acid amphiphilic peptide, GIGAVLKVLTTGLPALISWIKRKRQQ, which is as a prominent venom component in the honeybee *Apis mellifera*.[27] The toxic effect of melittin induces the lysis of red blood cells in the human bloodstream. Melittin is a highly soluble AMP (antimicrobial peptide) with a molecular weight of 2.86 KD with antitumor activity as well as the microbial action. Melittin has nonpolar residues such as Ile-17, Leu-6, Leu-13, Ile-2, Leu-9, Leu-

[a] *Department of Chemistry, University at Albany, State University of New York, 1400 Washington Ave, Albany, NY 12222, USA.*
[b] *Marketing Data Science, Expedia Group, 350 Fifth Ave, 7220, New York 10118.*
[c] *RNA Institute, University at Albany, State University of New York, 1400 Washington Ave, Albany, NY 12222, USA.*

† Footnotes relating to the title and/or authors should appear here.
Supplementary Information available: [details of any supplementary information available should be included here]. See DOI: 10.1039/x0xx00000x

16, Val-5 and Ile-20 on the hydrophobic side. The polar residues are Lys-21, Lys-7, Arg-22, Gln-25, Gln-26, Thr-10 and Thr-11, and Ser-18 are present on the hydrophilic side. The cationic residues Arg 24 and Lys 23 reside at the interface of hydrophilic and hydrophobic surfaces. The nonpolar residues as Ala-4, Ala-15, Pro-14 and Val-8 are aligned on the hydrophilic side. In aqueous solutions at low pH and with a low ion concentration of 0.01 M, melittin exists as a monomeric peptide that assumes a random coil conformation.[11, 28] The presence of lipid micelles or bilayers can induce assumption of an α-helical conformation by the peptide thereby enabling pore formation in membranes. Similarly, the addition of TFE as a cosolvent also triggers the adoption of an α-helical structure. The effect of cosolvents on the stability of the melittin α-helix has been investigated by different others using molecular simulation methods. It was found that in a TFE-water system melittin the experimentally observed α-helical structure was preserved, whereas in water the peptide began to bend and unfold.[7, 8, 15, 23, 29-31]

The utility of TFE as a cosolvent motivated the study of a novel hydrophobic fluorinated alcohol, 2-tetrafluoro(trifluoromethyl)-λ^6-sulfanylethan-1-ol (CF_3SF_4-ethanol).[25] CF_3SF_4-ethanol exhibited the properties akin to well-known fluorinated alcohols. The polar hydrophobicity associated with the CF_3SF_4 group was retained by CF_3SF_4-ethanol. In contrast with TFE, even though the more hydrophobic and lipophilic, CF_3SF_4-ethanol exhibits similar solution-phase dynamics and properties. CF_3SF_4-ethanol displayed a heightened propensity for aggregation at significantly lower concentrations. Due to this hydrophobicity-driven tendency to aggregate, CF_3SF_4-ethanol could serve as an excellent co-solvent for enhancing the stability of the secondary and tertiary structures of proteins and peptides in aqueous solutions. The amphiphilic nature of fluoroalcohols, characterized significant hydrophobicity, likely influences molecular structures. The electronegativity of fluorine increases the acidity of the OH group, rendering the alcohol an effective proton donor but a poor proton acceptor. This property results in the tendency of the fluoroalcohols to interact with a protein surface displacing the water that disrupts peptide intramolecular hydrogen bonds.

In this research, molecular dynamics simulations of melittin in both CF_3SF_4-ethanol-water and TFE-water systems enabled comparison of the effects of CF_3SF_4-ethanol relative to TFE. The role of Van der Waals interactions, differences in electrostatic energy, polar and non-polar solvation energies, and binding energy between the peptide backbone and alcohol molecules were examined to understand the mechanism by which these alcohols interact with melittin. Additional insights into the mechanism were derived from the intra-peptide and inter-molecular hydrogen bonding. Theoretical ellipticity and helicity were computed for the simulated systems to ascertain the helix stability. To tie our observations together, data from far UV circular dichroism measurements were collected to validate the molecular dynamics simulations with empirical data. Analyses indicated that the helicity of the peptide preserved with significantly lower concentrations of CF_3SF_4-ethanol than that required with TFE.

Experimental methods

Molecular dynamic simulations

The initial melittin conformation employed in the simulation experiments was taken from a 0.2-nm-resolution single crystal X-ray diffraction structure (PDB entry 2MLT).[32] The single crystal Xray diffraction structure is referred to as MLT throughout the paper. All simulations were performed using GROMACS (v2019.4).[33] The peptide was centered in a cubic box and solvated with two solvents-TIP4P water,[34] 8, 10, 20, 30, 40% (v/v) TFE-TIP4P water and 0.5, 1.0, 2.5, 4.5, 6 and 8% (v/v) CF_3SF_4-ethanol-TIP4P water. The solvent systems were randomly placed in an 11.6 nm^3 cube.[3] Here, we will focus our discussion on 1% and 8% CF_3SF_4-ethanol -water system, and 8% and 40% TFE-water system. The number of fluoroalcohol and water molecules involved in simulation are listed in Table 1.

Table 1: Total Number of Alcohol/waters used for Melittin simulation.

%(v/v)	$N_{TFE/water}$	$N_{CF3SF4\text{-}ethanol/water}$
0.5	-	50/51354
1.0	-	100/50979
2.5	-	200/50191
4.5	-	400/48690
6.0	-	500/47945
8.0	1000/47586	700/46653
10.0	1400/45872	1000/44147
20.0	2600/41118	-
25.0	3400/37954	-
30.0	4200/34973	-
40.0	5150/31526	-

All solvent molecules with any atom within 0.15 nm of the peptide were removed. Five chloride counter-ions were added to neutralize the total charge of the systems by replacement of water molecules at the most positive potential. The previously proposed models of the CF_3SF_4-ethanol and TFE, were utilized.[25] These models had been optimized to reproduce the physio-chemical properties of the pure liquid and aqueous solutions. The model was in good agreement with the experimental data derived from dynamic light scattering (DLS) experiments. OPLS-AA force field parameters were utilized.[25 35] All the systems were initially energy-minimized with the steepest descent method for 1000 steps followed by two 1 ns simulations of equilibration at NVT and NPT ensembles. During the MD simulations, the peptides and the rest of the systems were coupled separately with the temperature bath. The temperature was maintained at 300 °K by weak coupling to an external temperature bath using a coupling time t_T= 0.1 psec.[36] The simulations were performed at a constant pressure of 1 bar using the Parrinello-Rahman algorithm[37] with a relaxation time of 2 ps and isothermal compressibility of 4.5 x 10^{-5} bar.$^{-1}$ A stochastic velocity-rescaling thermostat was used to control the temperature with a 0.1 ps period.[38] Periodic boundary conditions were applied, with a cutoff of 1.4 nm used for short-range interactions. Long-range electrostatic interactions were calculated by the Particle-Mesh Ewald (PME)[37]

summation method with a fourth-order interpolation and a grid spacing of 0.16 nm. All bonds involving hydrogen atoms were constrained with the LINCS algorithm.[39] To integrate the equations of motion, the leap-frog algorithm was used with a time step of 2 fs. For the water molecules, the SETTLE algorithm[40] was applied. No reaction field corrections beyond the long-range cutoff were included in the cutoff simulations. Interactions within the short-range cutoff were updated at every time step, whereas interactions within the long-range cutoff were updated every five-time steps together with the pair-list. All atoms were given an initial velocity obtained from a Maxwellian distribution at the desired initial temperature. All the simulations were equilibrated by 50 ps of MD runs with positional restraints on the peptide to allow the relaxation of the solvent molecules. These first equilibration runs were followed by another 50-ps run without position restraints on the peptide. The production runs, after equilibration, were 50 ns long.

To prevent potential bias in understanding the mechanism from pre-folded helical structures (PDB:2MLT), we initiated our study with perturbed helical conformations obtained from melittin simulations in pure water.[32 41] The structure was validated by utilizing Chimera.[42] The perturbed structure of melittin (19.2% helicity) was denoted as RMLT throughout the paper. The partially unfolded structure that was obtained has only 19.2 % helicity. The same simulation systems were run with the above-mentioned parameters.

The secondary structure of the peptide was analyzed using the RMSD and RMSF tools from GROMACS.[33] The simulation trajectory file was read by *gmx do_dssp* tool.[33] The secondary structure was computed for each time frame over the course of the simulation. For this study, the secondary structure count with function of time achieves equilibrium in last 10 ns (S.I. Fig.S1-S4).

The time average of the α-helicity is reported for all the simulations by utilizing gmx_helix[33] tool. The local alcohol concentration was derived by gmx select tool, to obtain the number of water and alcohol molecules present around the peptide, within 0.6 nm.

H-bonding was calculated by gmx H-bond tool of GROMACS.[33] All simulation snapshots were generated by utilizing PyMOL software.[43]

Calculation of the free energy of binding

Calculation of the free energy of binding provides insight into the polar and nonpolar interactions between the peptide and the fluoroalcohols. The *g_mmpbsa* tool was used to calculate the free energy of binding by MM-PBSA method.[44,45] The total free energy of binding (ΔG) was computed by summing the difference of polar free energy (ΔG_{polar}) and the free energy of non-polar interactions ($\Delta G_{non-polar}$) which can be expressed as,

$$\Delta G_{Total} = \Delta G_{polar} + \Delta G_{non-polar} \quad (1)$$

ΔG_{polar} is summation of the electrostatic energy (ΔG_{elec}) and the polar solvation energy (ΔG_{ps})

$$\Delta G_{polar} = \Delta G_{elec} + \Delta G_{ps} \quad (2)$$

The difference of Van der Waals interaction (ΔG_{VdW}) and the difference of nonpolar solvation energy (ΔG_{nps}) summed up to contribute to the nonpolar binding energy.

$$\Delta G_{nonpolar} = \Delta G_{VdW} + \Delta G_{nps} \quad (3)$$

Circular dichroism

Melittin, obtained from Sigma-Aldrich, was purified by dialysis. To compare the effect of different fluoroalcohols, TFE and CF_3SF_4-ethanol, the far-UV CD spectra were measured with a Jasco spectropolarimeter at 20 °C with 1 mm pathlength cell. Samples of a stock solution of 1 mM melittin was prepared by dissolution in 10 mM HEPES (Sigma-Aldrich) and 0.5 M NaCl at a pH of 7.5. Samples were prepared from 20 µL of melittin stock solution and the appropriate volume of alcohol-buffer so that the melittin concentration was maintained across all the alcohol-water systems. TFE and CF_3SF_4-ethanol water systems were prepared at concentrations (% v/v) of 10 %, 20 %, 30 % and 40 %; and 0.5 %, 1 %, 2.5 %, 4.5 %, 6 %, 8.0 %, and 10 % respectively. Data were expressed as molar residue ellipticity (θ) which is defined as (θ) = 100 θ_{obs}/lc, where θ_{obs} is the observed ellipticity in degrees, c is the concentration in residue moles per liter, and l is the length of the light path in centimeters. Alcohol induced transitions are rapid, so the measurements were taken immediately after preparation of the solutions.

Calculation of peptide ellipticity

The theoretical circular dichroism (CD) spectra of the peptide in CF_3SF_4-ethanol and TFE as calculated with SESCA[46] and were compared with experimental results. Theoretical spectra were calculated with recommended basis set contributions of the backbone and side chains (DSSP-1SC3, DISICL-dTSC3, and HBSS-3SC1 bases set). The theoretical and experimental CD were in good agreement for the HBSS-3SC1 basis set for all calculations.

Result and discussion

Preservation of helicity

As indicated by the simulation snapshots shown in Fig. 1, the initial crystal structure of melittin (2MLT) utilized for MD simulation, after 10 ns in water, the peptide loses its helical structure and adopts a random coil conformation. This phenomenon has been extensively studied by others.[11, 15, 30, 47] When the peptide structure was simulated in CF_3SF_4-ethanol, the helix structure was preserved.(See S.I., Fig. S5) At lower CF_3SF_4-ethanol concentrations, in first 10 nanoseconds, the peptide lost the helical confirmation but at longer simulation times the structure regained helicity. At 8% concentrations of CF_3SF_4-ethanol, CF_3SF_4-ethanol aggregates readily around the peptide with no loss of helicity over the course of the simulation. The TFE-water system has similarly demonstrated the preservation of helicity over the course of the simulation. The simulation results for TFE-water closely replicated findings from previous studies (S.I., Fig. S6).

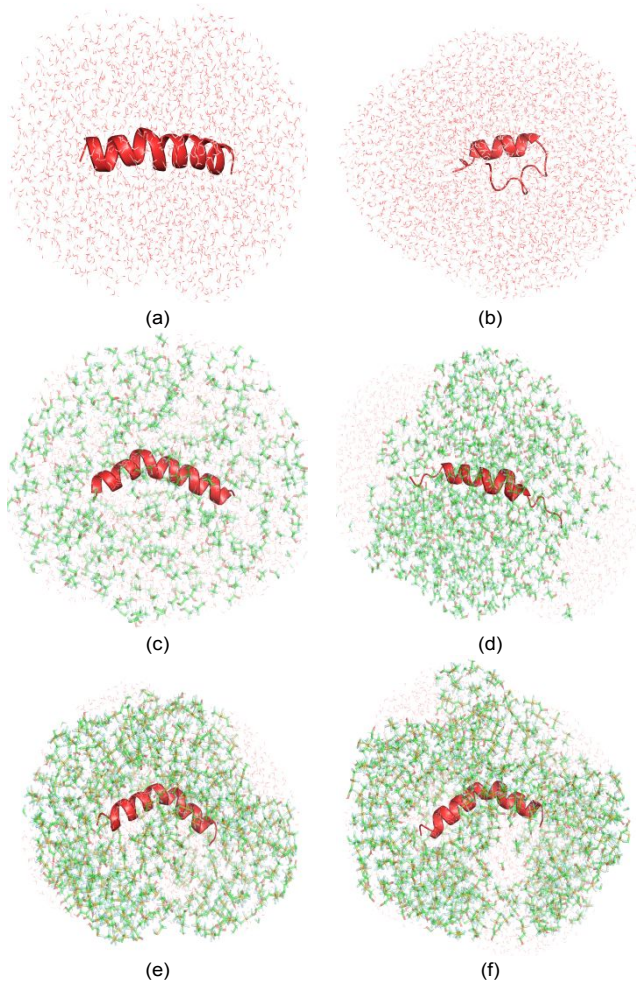

Figure 1. Representative snapshot of simulation within a distance of 0.6 nm from the melittin backbone a) PDB: 2MLT of crystal melittin in pure water at the beginning of simulation, b) random coil structure of melittin after 50 ns simulation in water system, c) PDB: 2MLT of melittin in 40% TFE-water system at the beginning of simulation, d) α-helix of melittin after 50 ns simulation in 40%TFE-water system, e) PDB: 2MLT of melittin in 8% CF_3SF_4 -ethanol at the beginning of simulation and f) α-helix of melittin after 50 ns simulation in 8% CF_3SF_4-ethanol-water system.

Promotion of helicity

To better understand how fluoroalcohols influence the transition from a random coil structure to a helical conformation, the simulation studies were extended to begin with melittin in a random coil. Pre-folded helical initial structures (PDB:2MLT) could bias the mechanistic investigation, whereas perturbed helical conformations could overcome this bias. The partially unfolded starting conformation (19.2 % helicity) (RMLT) was known to perturb the helical structure of melittin[41,32] when the OPLS-AA force field was used.

Experimental evidence was strongly supportive of the role of fluoroalcohols in helix stabilization.[1,3,4,13,14,18, 20,21] Computational analyses were necessary to provide the mechanistic details at the molecular level. The simulations were performed at a series of different fluoroalcohol concentrations (S.I. Fig. 7. and 8). It was found that mixtures of 1 % and 8 % CF_3SF_4- ethanol concentrations was particularly informative.

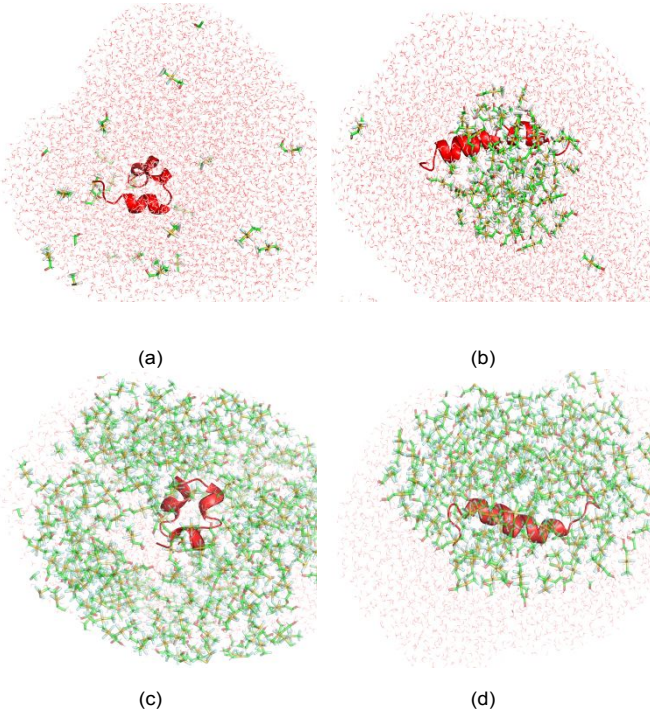

Figure 2. Representative snapshot of simulation within a distance of 0.6 nm from the melittin backbone a) random coil structure of melittin(RMLT) in 1% CF_3SF_4-ethanol-water system at the beginning of simulation; b) α-helix of melittin after 50 ns simulation in 1% CF_3SF_4-ethanol -water system; c) random coil structure of melittin in 8% CF_3SF_4-ethanol -water system at the beginning of simulation; d) α-helix of melittin after 50 ns simulation in 8% CF_3SF_4-ethanol-water system.

In 1 % of CF_3SF_4-ethanol aqueous solutions, melittin assumed the α-helical structure shown in Fig. 2(d). At 8 % of CF_3SF_4-ethanol, melittin had a very high helicity (Fig. 3 (h)). In contrast with the newly synthesized alcohol, simulations at 8 % and 40 % by volume TFE-water were investigated. At 8 % TFE, the peptide does not regain helicity,as shown in Fig. 3 (b), however at 40 % TFE concentration the peptide reaches the highest helicity (Fig. 3 (d)).

Simulation times of 50 ns were used to model systems with 1 % and 8 % by volume of CF_3SF_4-ethanol-water and 8 % and 40 % by volume TFE respectively (See S.I., Fig. 9). The RMSD of melittin backbone in each system was compared with the peptide backbone fluctuation that occurred in pure water.(See S.I., Fig. S10-S13) In each system, the fluctuation of the peptide backbone in the fluoroalcohols is lower than in that which occurs in pure water. In Fig. SCC, with CF_3SF_4-ethanol, in as low as 1 % by volume and at higher concentration, 8 % by volume, the “plateau” (convergence in 50 ns) was achieved.

To confirm the relative convergence of the backbone movement invoked at 50 ns, the simulation was extended to 100 ns. (See S.I., Fig. S11) The results from the additional simulation time are consistent with those found at 50 ns.(For additional insights please see S.I., Fig. S14, a video that clearly illustrates the motion of the melittin backbone on exposure to 8 % CF_3SF_4- ethanol.) The structure stabilizes with an RMSD around 0.7 for last 10 ns. On the other hand, in water, the increase of RMSD values to 0.98 nm over the course of the simulation is indicative of the loss of helicity over time. In case of

water, the plateau for last 10 ns is consistent with the equilibrated state of random coil structure of melittin.

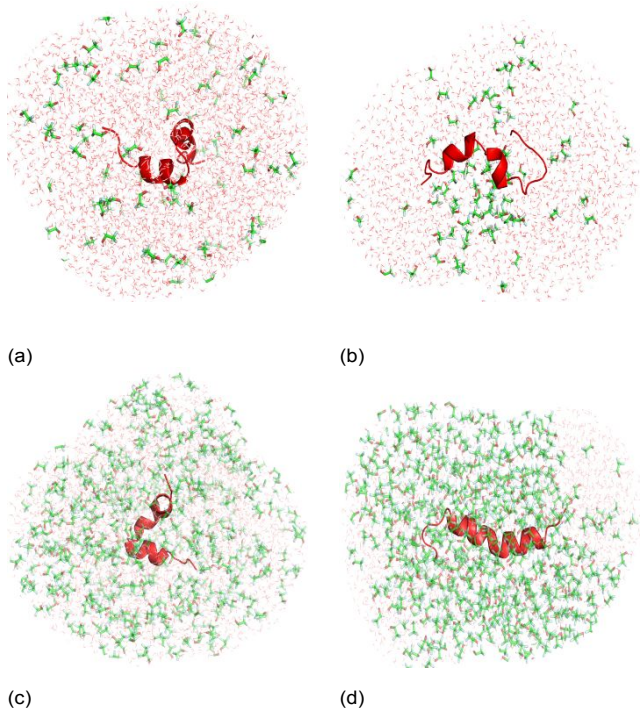

Figure 3. Representative snapshot of simulation within 0.6 nm from the melittin backbone a) random coil structure of melittin (RMLT) in 8% TFE-water system at the beginning of simulation b) α-helix of melittin after 50 ns simulation in 8% TFE-water system c) random coil structure of melittin in 40% TFE-water system at the beginning of simulation d) α-helix of melittin after 50 ns simulation in 40% TFE -water system.

In TFE at the lower concentration of 8 % by volume convergence never occurs. This is consistent with the inability of TFE to stabilize the helical structure at a volume as low as a concentration of CF_3SF_4-ethanol of 1 %. At 40 % by volume of TFE, after 20 ns, the structure stabilizes at 0.8 nm. RMSD calculation establishes that the helices deform in water, but the peptide is more stable in the presence of TFE or CF_3SF_4-ethanol.

Root mean square fluctuation (RMSF).

RMSF, the root mean square fluctuation, a measure of individual residue flexibility or how much a particular residue moves (fluctuates) during a simulation was plotted vs. residue number at various alcohol concentrations. The RMSF findings established that the peptide residues in water have higher fluctuations than when the peptide is exposed to various TFE and CF_3SF_4-ethanol concentrations. In S.I. Fig. S15, it is evident that the hydrophobic side chains of RMLT peptide backbone fluctuate most in water from 0.3 to 0.8 nm. In 1 % CF_3SF_4-ethanol, the fluctuation ranges from 0.2 to 0.6 nm, and in 8% CF_3SF_4-ethanol the movement is on average of 0.17-0.6 nm. On the other hand, in 8% by volume of TFE, the fluctuations are closer to those found with CF_3SF_4-ethanol solutions. It is noteworthy that in CF_3SF_4-ethanol solutions, the hydrophobic sidechains, represented by residue numbers 2, 4, 5, 6, 8, 9, 13, 15, 16, 17 and 20 have fewer fluctuations.[11,7] The probable hydrophobic interactions between the hydrophobic side chains of peptides and highly hydrophobic functional CF_3SF_4 group of CF_3SF_4-ethanol,[25] play an important role in stabilizing the secondary structure of the peptide.[21] The *N*-terminal and *C*-terminal segments of the peptide were observed to exhibit flexibility.[18] (See S.I. Figs. S13-S16) This flexibility can be attributed to the absence of neighboring amino acids that would otherwise constrain the movement of the terminal segments.

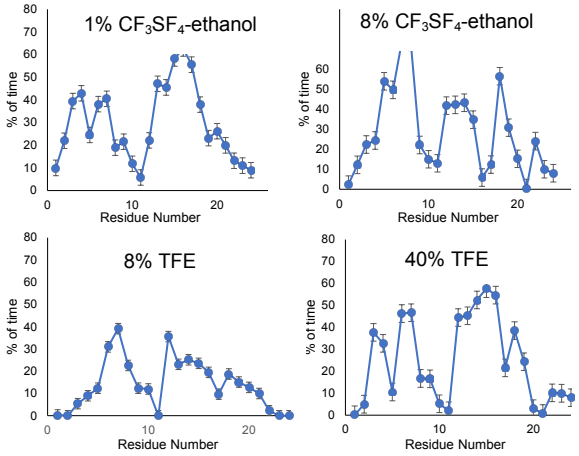

Figure 4. Time average of α-helicity per residue of Melittin for last 10 ns of equilibrated simulation in 1%, and 8% CF_3SF_4-ethanol-water and 8% and 40% TFE-water system with respect to residue number.

Time average of the α-helicity of secondary structure.

The time average of the α-helicity is reported for TFE and CF_3SF_4-ethanol in Fig. 4. (see also S.I. Figs. S20-S23) An extensive NMR spectroscopic analysis of melittin's structure in a fluoroalcohol/water environment revealed the presence of a bent structure with two fluctuating α-helices in melittin.[30] The boundaries of the first helix are between amino acids 3 and 8 for the TFE and CF_3SF_4-ethanol simulations. The second helix starts at residue 12 for the TFE and CF_3SF_4-ethanol and it extends up to residue 24.

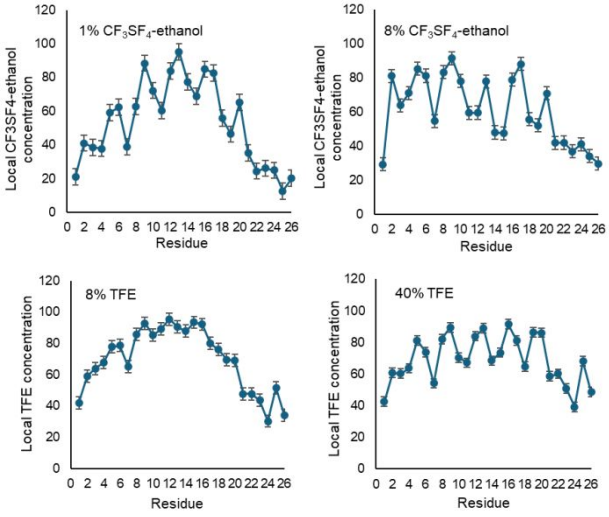

Figure 5. The influence of increasing alcohol concentration on local TFE and CF_3SF_4-ethanol concentration around individual melittin residues.

Local Alcohol Concentration around the peptide.

The fluoroalcohols were placed randomly around melittin in the simulation box. During the simulation the alcohols interact with one and another through strong hydrogen bonding interactions that results in aggregation.[25,9] These simulations indicate accumulation of the fluoroalcohols around melittin is site-specific. The concentration of CF_3SF_4-ethanol molecules was higher in the regions of the hydrophobic side chains than the areas around the hydrophilic side chains. Previous studies have shown the aggregation of TFE molecules around the region of the peptide in turn stabilized the secondary structure of melittin. Similar to TFE, CF_3SF_4-ethanol molecules aggregate around the solute preventing the formation of hydrogen bonds with water that can disrupt an α-helical structure.[7, 11, 48, 49] The interactions between the peptide and CF_3SF_4-ethanol do not displace the peptide–peptide interactions that stabilize the secondary structure. In the case of CF_3SF_4-ethanol, the greater occuppied volume can further minimize the possible interactions of CF_3SF_4-ethanol with the backbone melittin atoms, enhancing the α-helix stabilization.

The origins of stabilization may be both entropic and enthalpic. It was determined the hydrophobic cosolvent tends to cluster around regions of the peptide that are rich in hydrophobic side chains (Fig. 5). This effect tends to displace ordered water molecules from the vicinities of both fluoroalcohols and the hydrophobic side chains of the peptide. The increased concentration of fluoroalcohols surrounding the hydrophobic side chains of the amino acids notably contributed to the occurrence of helicity. The hydrophobic side chains of residue numbers 2, 4, 5, 6, 8, 9, 13, 15, 16, 17, and 20 acted as anchors, are embedded within the alcohol aggregates. These interactions had the effect of reducing the fluctuations. This phenomenon demonstrates how the alignment of hydrophobic residues within the alcohol aggregates plays a crucial role in the stabilization of the helical structure. The concentration of CF_3SF_4-ethanol and TFE molecules around the peptide residues, that is the local alcohol concentration (LAC), was established by determining the total number of water molecules $n_W(r)$ and fluoroalcohol $n_H(r)$ molecules present within a distance r from the α-carbons of individual amino acid residues using the following relation:[7, 11]

$$LAC(r) = \frac{V_m^H n_H(r)}{V_m^H n_H(r) + V_m^w n_w(r)} \times 100 \quad (4)$$

where V_m^H= 0.1 and V_m^w= 0.019 L/mol are the average excluded volumes for alcohol and water molecules, respectively.[7] The local CF_3SF_4-ethanol molecule concentration (LAC) around a hydrophobic residue are in range of 57-90 % and 71-92 % at 1 % and 8 % CF_3SF_4-ethanol by volume respectively. The CF_3SF_4-ethanol concentration around the hydrophilic side chain is around 12 % and 29 %, respectively. In the case of TFE, at lower concentrations, TFE is abundant around both the hydrophilic and hydrophobic side chains of the peptide. On the contrary in 40% TFE, the TFE molecules clustered around the hydrophobic side chain in 63-92% concentration. It can be argued that the more hydrophobic CF_3SF_4-ethanol interacts more strongly with the hydrophobic side chains of melittin, particularly at low concentrations. In contrast at low TFE concentrations, there is evidence for more amphipathic behavior.

Intrapeptide and intermolecular hydrogen bonding.

Once water is excluded from the immediate environment of the peptide, intra-molecular hydrogen bonds can form. To learn more about the interactions between the peptide and the alcohols, the number of hydrogen bonds between the alcohols and between peptides and the water molecules was determined. The structure of an alpha helix is maintained by a network of hydrogen bonds between the carboxyl oxygen of the peptide backbone and amino group of 4th next amino acid (n to n+4) in the primary structure. The number of hydrogen bonds formed during the simulation was computed with the GROMACS H-bond tool. A cutoff value of 0.3 nm for the distance between acceptor and donor and the cut off angle of 120° was established. In CF_3SF_4-ethanol solutions the network of hydrogen bonds between the carboxyl oxygen of the backbone and amino group of 4th next amino acid (n to n+4) forms more hydrogen bonds than it is in TFE alcohol solutions. (Fig. 6 (a), (b), (c)). The average number of intrapeptide H-bonds in 1% CF_3SF_4-ethanol is 9.02, 8% CF_3SF_4-ethanol is 9.94 whereas in 8 %TFE 4.31 and 40% TFE is 4.82. Intra peptide H-bonds determine the stability of an α-helix. In water, the number of hydrogen bonds significantly decreases as the highly ordered structure of the crystal structure is denatured and then upon partial refolding the number of in intrapeptide bonds increases with partial recovery of helicity as seen in RMLT. Additionally, previous research has demonstrated the formation of strong intermolecular hydrogen bonds between water and melittin lead to a loss of the α-helical structure.[23, 50] The loss of helical peptide structure can be driven by the formation of intermolecular hydrogen bonds between the peptide backbone and the water.[47] Fig. 6 (d) and (e) show the number of intermolecular H-bonds in 8 % in CF_3SF_4-ethanol-water and 40 % TFE-water system decreases in the presence of alcohol molecules than it is in pure water. In pure water, the number of intermolecular H-bonds range between 35-40 and in TFE-water the number is in the 18-20 range. In the CF_3SF_4-ethanol-water system, a more substantial decrease was observed, ranging from 14 to 18 hydrogen bonds. This decrease can be attributed to the potential steric hindrance that results from the steric demand of CF_3SF_4-ethanol molecules around the peptide. This hindrance could limit the accessibility of water molecules to the peptide's surface.(Fig. 7) The influence of the alcohol concentration and hydrogen bonding between the alcohol and the peptide is shown in Fig. S24. There is little to no change in hydrogen bonding between the alcohol and the peptide with increasing alcohol concentration.

PAPER

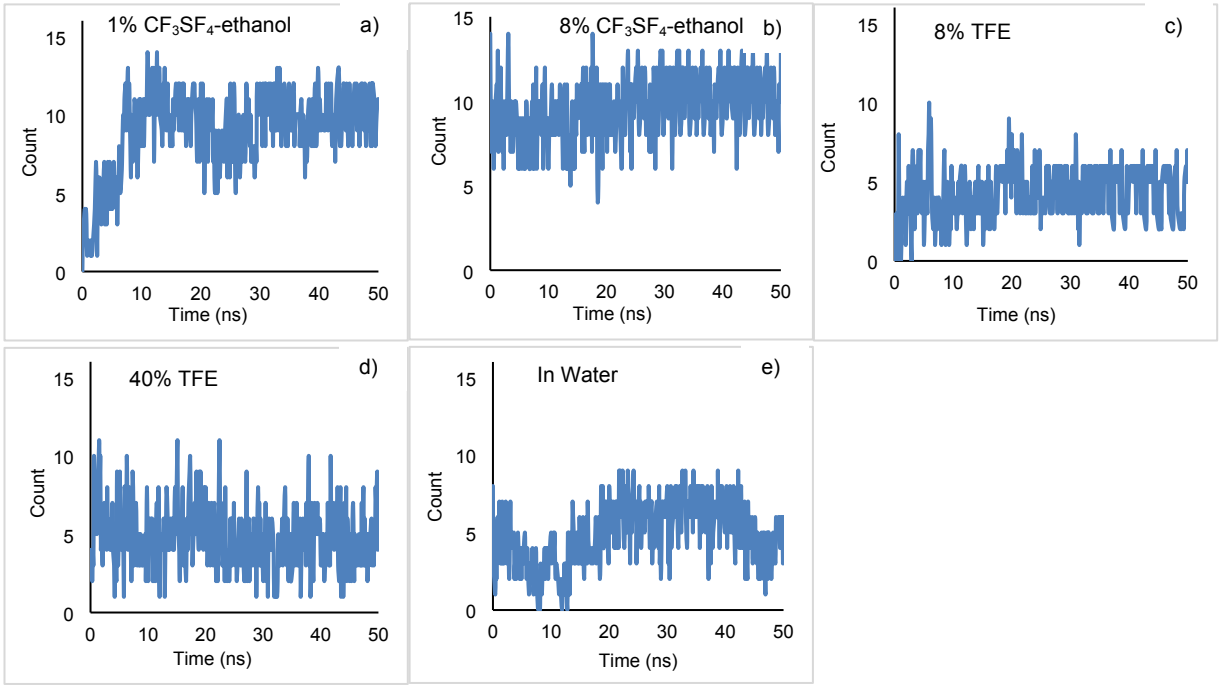

Figure 6. Intra-peptide H-bonding in melittin in presence of a) 1% CF_3SF_4-ethanol, b) 8% CF_3SF_4-ethanol, c) 8% TFE, d) 40% TFE and e) pure water.

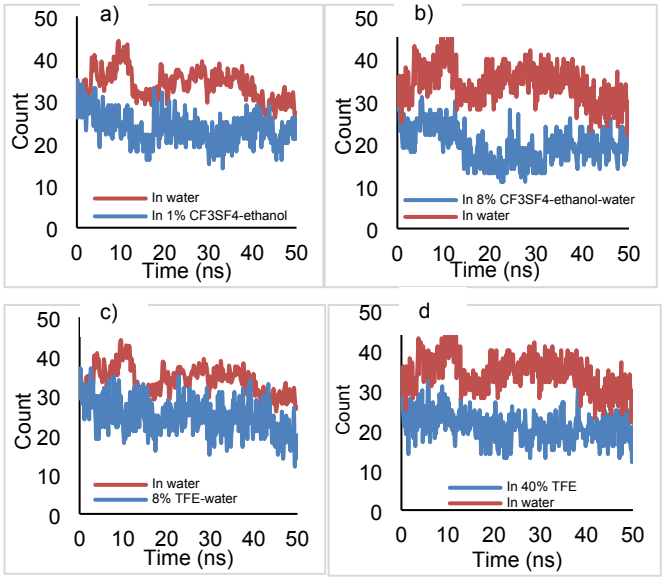

Figure 7. Inter molecular H bonding between water and peptide in a) 1% CF_3SF_4-ethanol, b) 8% CF_3SF_4-ethanol, c) 8% TFE, and d) 40% TFE

The free energy of binding calculation.

The stabilization of secondary structure by fluoroalcohols established the contribution of different interactions. Those interactions include Van der Waals, hydrophobic and electrostatic interactions, polar and SASA energy, as well as H-bonding. The computation and decomposition of the free energy of binding, ΔG_{bind}, between the peptide and fluoroalcohols can be determined using MMPBSA (Molecular Mechanics-Poisson Boltzmann Surface Area) method.[44,45] In MM-PBSA methods, the free energy of binding was estimated from molecular mechanical energies and solvation free energies for an ensemble of molecular configurations to include water, aqueous fluoroalcohols in the presence of melittin can be obtained from molecular dynamics simulations. The energetics underlying the binding of fluoroalcohols, and the peptide obtained from MMPBSA calculations are listed in Table 2 that lists the summary of energies for 8 % CF_3SF_4-ethanol and 40 % TFE.

The total free energy of binding has values between -725.3 KJ / mol and -629.9 KJ / mol and the intermolecular electrostatic interactions are -467.5 KJ / mol and -288.6 KJ / mol respectively for CF_3SF_4-ethanol and TFE water systems. The contributions that favor binding are Van der

Table 2. Energy Contributions in KJ / mol for 1%, 8% CF_3SF_4-ethanol and 8%, 40% TFE in simulation.

	1% CF_3SF_4-ethanol	8% CF_3SF_4-ethanol	8% TFE	40% TFE
VdW Energy[a]	-620.1	-607.2	-590.2	-582.4
Electrostatic Energy[a]	-460.2	-467.5	-300.5	-288.6
Polar Solvation Energy[a]	440.7	442.0	350.5	320.7
SASA Energy[a]	-90.2	-92.6	-85.3	-79.6
Binding Energy[a]	-710.0	-725.3	-650.1	-629.9

a. KJ/mol

Waals interactions between the interacting partners in the range of -607.22 KJ / mol and -582.4 KJ / mol for CF_3SF_4-ethanol and TFE water systems respectively. The nonpolar interactions with the solvent including the contribution from the hydrophobic effect yield contributions in the range of -92.5 KJ / mol for CF_3SF_4-ethanol and -79.6 KJ / mol for TFE, which is opposed by an unfavorable desolvation of polar groups yielding contribution of 442.0 KJ / mol and the 320.7 KJ / mol for CF_3SF_4-ethanol and TFE respectively. The Van der Waals energy and nonpolar interactions are more favorable in CF_3SF_4-ethanol than in TFE. The simulations indicate that the OH group of fluoroalcohols have electrostatic interactions with amino groups of melittin.

This analysis was also used to estimate the free energy of binding and the contributions of each amino acid in the interactions between melittin and fluoroalcohols. This method utilizes a series of optimized snapshots of the trajectory to calculate the contribution to the overall energy. The result is represented in Fig. 8. From all simulations the nonpolar residues contribute more to the peptide alcohol interactions and are responsible for stabilization of secondary structure of melittin.

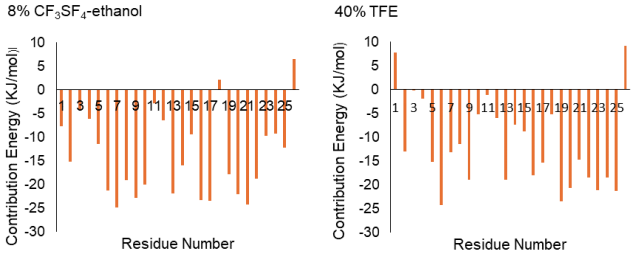

Figure 8. Representation of contribution energy in 8% CF_3SF_4-ethanol-water and 40% TFE-water system with respect to melittin residue.

Circular dichroism (CD) experiment.

In neat buffer, low ionic strength and a melittin concentration of 1.0 mM, the peptide predominantly exists in monomeric random coil structure. Melittin becomes dissociated to a monomer with the addition of TFE, CF_3SF_4-ethanol as cosolvent. The helical secondary structure of melittin was maintained by introduction of fluorinated alcohols was confirmed using circular dichroism (Fig. 9). The minima at 208 nm and 222 nm are characteristics of α–helices. Small additions of

b.

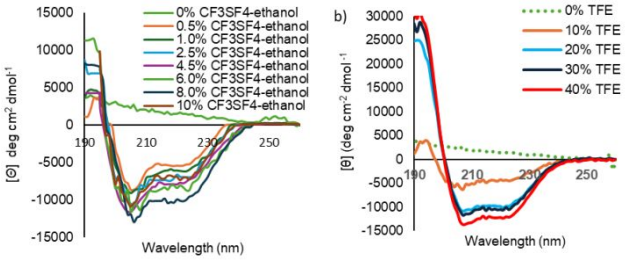

Figure 9. Far UV CD spectra of melittin for a) CF_3SF_4-ethanol-water system and b) TFE-water system.

CF_3SF_4-ethanol even as little as 0.5 % (v/v) as cosolvent the helical content increased slightly, as shown in Fig. 11 (a). The gradual addition of a synthetic alcohol can disturb the

random coil structure and promote the α-helical monomer. The α-helical secondary structure remained stable with 0.5-8.0 % by volume solutions of CF_3SF_4-ethanol and decreases with 10 % CF_3SF_4-ethanol. The decrease in helicity observed in computational analysis[25] of solutions of 10 % CF_3SF_4-ethanol likely results in phase separation.

These results indicate that CF_3SF_4-ethanol and other fluorinated alcohols surround the peptide because of a propensity to aggregate. As reported by other researchers, the highest helicity in melittin is found in 40 % (v/v) of TFE and has been validated by the findings from CD measurements.[1]

Circular dichroism determination by SESCA.

The α-helical melittin structures in TFE-water and in CF_3SF_4-ethanol-water system obtained from 50 ns simulation were employed in SESCA computed circular dichroism (CD) spectra.[46,26] The calculated CD spectra were compared with the experimental results. There was no difference in the theoretical helicity computed from the 100 ns simulation and the 50 nanosecond experiment. SESCA can successfully extract information for CD spectra and is especially informative in establishing a quantitative link between structural configuration and the observed spectra.

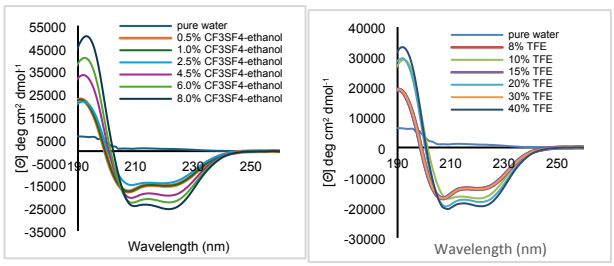

Figure 10. Theoretically calculated CD spectra of melittin for a) CF_3SF_4-ethanol-water system and b) TFE-water system.

The effects of conformational flexibility are addressed using structural ensembles during CD predictions that consider the contribution of natural amino acid side chains. Inclusion of these contributions increases the prediction accuracy. In Fig. 10 the similarity between our experimental and theoretical CD results can be seen.

Comparison in helicity calculation.

The helicity was calculated from both the experimental and theoretical circular dichroism findings. For helicity calculations, ellipticity data at 222 nm where helical structure exhibits a characteristic minimum in ellipticity,[22] are commonly used to quantify the helical content of protein (i.e., 222 nm method). The α-helix content was calculated based on the algorithm developed for coiled-coil proteins developed by Holtzer et al. [51]

$$\Phi_h = \theta - \theta_c + \frac{2.55\, I\,(\theta_{h\infty})}{\mathrm{n}(\theta - \theta_{h\infty})} \qquad (5)$$

where, Φ_h = fraction of residues in an α-helical conformation, $\theta_{h\infty}$ = mean residual ellipticity at 222 nm for α-helix of infinite length, θ_c = mean residual ellipticity for a random coil at 222 nm, I is the average number of helical segments per chain, n is the number of peptide bonds, and q is the mean residual ellipticity at 222 nm. The calculated helicities determined by the are in good agreement with those experimentally. (See Table 3)

Table 3. Comparison between helicity of melittin obtained from experimental and calculated by SESCA in 8% and 40% TFE and 1% and 8% CF_3SF_4-ethanol.

Helicity Alcohols at 222 nm			
Alcohol	Concentration (v/v) [a]	Experimental Helicity[a]	Theoretical Helicity[a]
TFE	40	53	54
TFE	8	19	22
CF_3SF_4-ethanol	1	37	42
CF_3SF_4-ethanol	8.0	54	62%

a. In percent

Conclusions

CD experiments and molecular dynamics simulations of the influence of aqueous solutions of CF_3SF_4-ethanol and aqueous solutions of TFE show consistent results. In water, melittin assumes a random coil conformation. However, on exposure to aqueous CF_3SF_4-ethanol, the helical structure of melittin stabilizes, even at concentrations as low as 1% CF_3SF_4-ethanol in water. The highest helical content for melittin occurs with concentrations of 8% by volume CF_3SF_4-ethanol. In contrast, TFE added to water does not induce the assumption of a helical structure at 8% concentration. The folding of melittin to assume a helical conformation requires the addition of 40% by volume of TFE to achieve maximum helicity for melittin. These findings were consistent with published findings.

The calculations of RMSD and RMSF provide insights into fluctuations of the peptide backbone when exposed to pure water, CF_3SF_4-ethanol-water, and TFE-water. Fluoroalcohols stabilize the hydrophobic side chain residues of melittin, and consequently promote the assumption of helical structure. Calculation of local alcohol concentrations around the peptide reveal concentrations ranging as high as 70-90% near the hydrophobic side chains of melittin. These concentrations lead to increased hydrophobic interactions between the peptide and fluoroalcohols, thereby displacing water molecules from the surface of the peptide. Disruption of water-peptide intermolecular H-bonding is a critical factor in driving peptide folding.

Both TFE and CF_3SF_4-ethanol promote intramolecular-peptide H-bonding, stabilizing helix formation. Fluoroalcohols engage in various interactions, including Van der Waals, hydrophobic, electrostatic, polar, and H-bonding. Using the MMPBSA method, the binding free energy, ΔG_{bind}, was calculated for the interactions between the peptide and fluoroalcohols. Our findings suggest that nonpolar residues play a major role in peptide-alcohol interactions and are key to stabilizing melittin's secondary structure. Emphasizing the importance of hydrophobicity, the SESCA method was used to derive the helicity of melittin from the simulated system and to validate those findings with experimental outcomes. CD results for melittin in TFE align with past findings and validate the role of CF_3SF_4-ethanol to bolster helicity. The experimental and calculated helicities are closely aligned. CF_3SF_4-ethanol is an eco-friendly option for enhancing the helical structure of peptides and proteins, even at concentrations as low as 1%.

Author contributions

Samadrita Biswas: Conceptualization, Methodology, Writing – Original Draft, Data Curation, Investigation, Visualization. **Nilavra Pathak:** Visualization**,** Software, Writing – Review & Editing. **Leah Sutherland:** Data Curation **Alan A Chen** – Supervision, Writing – Review & Editing, Funding Acquisition. **John T Welch** - Supervision, Writing – Review & Editing, Resources, Project Administration, Funding Acquisition.

Conflicts of interest

"There are no conflicts to declare".

Data availability

A data availability statement (DAS) is required to be submitted alongside all articles. Please read our full guidance on data availability statements for more details and examples of suitable statements you can use.

Acknowledgements

AC gratefully acknowledges the support of NSF-MCB 1651877 and JTW gratefully acknowledges the support of NSF-CHE 1464936 and NSF-CHE 2154772.We appreciate our laboratory members for thoughtful discussions and suggestions, and their time in reading and reviewing this work.

Uncategorized References

1. N. Hirota, K. Mizuno and Y. Goto, *J. Mol. Biol.*, 1998, **275**, 365-378.
2. T. To, Y. Sakamoto, K. Sadakane, M. Matsugami and T. Takamuku, *J. Phys. Chem. B*, 2021, **125**, 240-252.
3. B. Biswas and P. C. Singh, *J. Fluorine Chem.*, 2020, **235**, 109414.
4. M. S. Zaroog and S. Tayyab, *Process Biochem. Int.*, 2013, **48**, 853-862.
5. S. Bucciarelli, E. S. Sayedi, S. Osella, B. Trzaskowski, K. J. Vissing, B. Vestergaard and V. Foderà, *J. Colloid Interface Sci.*, 2020, **561**, 749-761.
6. H. Ohgi, H. Imamura, T. Sumi, K. Nishikawa, Y. Koga, P. Westh and T. Morita, *Phys. Chem. Chem. Phys. B*, 2021, **23**, 5760-5772.
7. D. Roccatano, M. Fioroni, M. Zacharias and G. Colombo, *Protein Science*, 2005, **14**, 2582-2589.
8. A. Das and C. Mukhopadhyay, *J. Chem. Phys.*, 2007, **127**.
9. J. T. Gerig, *J. Phys. Chem. B*, 2014, **118**, 1471-1480.
10. J. T. Gerig, *J. Phys. Chem. B*, 2015, **119**, 5163-5175.
11. D. Roccatano, G. Colombo, M. Fioroni and A. E. Mark, *Proc. Natl. Acad. Sci.*, 2002, **99**, 12179-12184.
12. S. Mondal, B. Biswas, T. Nandy and P. C. Singh, *J. Phys. Chem. B*, 2018, **122**, 6616-6626.
13. A. T. Alexandrescu, K. Rathgeb-Szabo, W. Jahnke, T. Schulthess, R. A. Kammerer and K. Rumpel, *Protein Sci.*, 1998, **7**, 389-402.
14. L. R. Brown, J. Lauterwein and K. Wüthrich, *Biochim. Biophys. Acta, Protein Struct.*, 1980, **622**, 231-244.
15. M. Fioroni, M. D. Diaz, K. Burger and S. Berger, *J. Am. Chem. Soc.*, 2002, **124**, 7737-7744.
16. E. F. Haney, H. N. Hunter, K. Matsuzaki and H. J. Vogel, *Biochim. Biophys. Acta, Biomembr.*, 2009, **1788**, 1639-1655.
17. G. D. Henry and B. D. Sykes, in *Methods Enzymol.*, Academic Press, 1994, vol. 239, pp. 515-535.
18. M. D. Kemple, P. Buckley, P. Yuan and F. G. Prendergast, *Biochemistry*, 1997, **36**, 1678-1688.
19. J. Lauterwein, L. R. Brown and K. Wüthrich, *Biochim. Biophys. Acta, Protein Struct.*, 1980, **622**, 219-230.
20. Y. Miura, *The Protein Journal*, 2022, **41**, 625-635.
21. A. J. Weaver, M. D. Kemple and F. G. Prendergast, *Biochemistry*, 1989, **28**, 8624-8639.
22. Y. Wei, A. A. Thyparambil and R. A. Latour, *Biochim. Biophys. Acta*, 2014, **1844**, 2331-2337.
23. M. Pezzella, K. El Hage, M. J. M. Niesen, S. Shin, A. P. Willard, M. Meuwly and M. Karplus, *J. Phys. Chem. B*, 2020, **124**, 6540-6554.
24. W. Wilcox and D. Eisenberg, *Protein Sci.*, 1992, **1**, 641-653.
25. S. Biswas, S. Kaur, C. A. Myers, A. A. Chen and J. T. Welch, *ACS Omega*, 2023.
26. A. F. Pereira, V. Piccoli and L. Martínez, *J. Mol. Liq.*, 2022, **365**, 120209.
27. E. Habermann, *Science*, 1972, **177**, 314-322.
28. R. M. S. Terra, J. A. Guimarães and H. Verli, *J. Mol. Graphics Modell.*, 2007, **25**, 767-772.
29. V. Daggett, *Acc. Chem. Res.*, 2002, **35**, 422-429.
30. J. T. Gerig, *Biophys. J.*, 2004, **86**, 3166-3175.
31. D. Schubert, G. Pappert and K. Boss, *Biophys. J.*, 1985, **48**, 327-329.
32. M. Andersson, J. P. Ulmschneider, M. B. Ulmschneider and S. H. White, *Biophys. J.*, 2013, **104**, L12-14.
33. H. J. C. Berendsen, D. van der Spoel and R. van Drunen, *Comput. Phys. Commun.*, 1995, **91**, 43-56.
34. W. L. Jorgensen, J. Chandrasekhar, J. D. Madura, R. W. Impey and M. L. Klein, *J. Chem. Phys.*, 1983, **79**, 926-935.
35. W. L. Jorgensen and J. Tirado-Rives, *J. Am. Chem. Soc.*, 1988, **110**, 1657-1666.
36. H. J. C. Berendsen, J. P. M. Postma, W. F. van Gunsteren, A. DiNola and J. R. Haak, *J. Chem. Phys.*, 1984, **81**, 3684-3690.
37. M. Parrinello and A. Rahman, *Phys. Rev. Lett.*, 1980, **45**, 1196-1199.
38. B. H. Paul Bauer, & Erik Lindahl. (2022). GROMACS 2022 Source code (Version 2022). Zenodo . https://doi.org/10.5281/zenodo.6103835.
39. B. Hess, H. Bekker, H. J. C. Berendsen and J. G. E. M. Fraaije, *J. Comput. Chem.*, 1997, **18**, 1463-1472.
40. S. Miyamoto and P. A. Kollman, *J. Comput. Chem.*, 1992, **13**, 952-962.
41. C. Liao, M. Esai Selvan, J. Zhao, J. L. Slimovitch, S. T. Schneebeli, M. Shelley, J. C. Shelley and J. Li, *J. Phys. Chem. B*, 2015, **119**, 10390-10398.
42. E. F. Pettersen, T. D. Goddard, C. C. Huang, G. S. Couch, D. M. Greenblatt, E. C. Meng and T. E. Ferrin, *J. Comput. Chem.*, 2004, **25**, 1605-1612.
43. W. L. DeLano and S. Bromberg, *DeLano Scientific LLC*, 2004, **629**.
44. R. Kumari, R. Kumar and A. Lynn, *J. Chem. Inf. Model.*, 2014, **54**, 1951-1962.
45. N. A. Baker, D. Sept, S. Joseph, M. J. Holst and J. A. McCammon, *Proc. Natl. Acad. Sci. U. S. A.*, 2001, **98**, 10037-10041.
46. G. Nagy, M. Igaev, N. C. Jones, S. V. Hoffmann and H. Grubmüller, *J. Chem. Theory Comput.*, 2019, **15**, 5087-5102.

47. A. Kitao, F. Hirata and N. Gō, *Chem. Phys.*, 1991, **158**, 447-472.
48. V. S. Pande, A. Y. Grosberg, T. Tanaka and D. S. Rokhsar, *Curr. Opin. Struct. Biol.*, 1998, **8**, 68-79.
49. R. Walgers, T. C. Lee and A. Cammers-Goodwin, *J. Am. Chem. Soc.*, 1998, **120**, 5073-5079.
50. J. T. Gerig, *J. Phys. Chem. B*, 2020, **124**, 9793-9802.
51. A. A. Paulucci, L. Hicks, A. Machado, M. T. Miranda, C. M. Kay and C. S. Farah, *J. Biol. Chem.*, 2002, **277**, 39574-39584.

Data Availability Statement

Influence of aqueous solutions of 2-(tetrafluoro(trifluoromethyl)-λ^6-sulfanyl-ethan-1-ol (CF_3SF_4-ethanol) on the stabilization of the secondary structure of melittin: Comparison with aqueous trifluoroethanol using molecular dynamics simulations and circular dichroism experiments.

Samadrita Biswas,*[a] Nilavra Pathak [b], Leah Sutherland[a], Alan A Chen[c] and John T Welch [a]

The data supporting this article have been included as part of the Supplementary Information.